

Two-dimensional Synchrotron Beam Characterisation from a Single Interferogram

Bojan Nikolic*

Cavendish Laboratory, University of Cambridge, Cambridge CB3 0HE, UK

Christopher L. Carilli

National Radio Astronomy Observatory, P. O. Box 0, Socorro, NM 87801, US

Nithyanandan Thyagarajan

*Commonwealth Scientific and Industrial Research Organisation (CSIRO),
Space & Astronomy, P. O. Box 1130, Bentley, WA 6102, Australia*

Laura Torino and Ubaldo Iriso[†]

*ALBA - CELLS Synchrotron Radiation Facility
Carrer de la Llum 2-26,
08290 Cerdanyola del Vallès (Barcelona), Spain*

(Dated: 17 May 2024)

Double-aperture Young interferometry is widely used in accelerators to provide a one-dimensional beam measurement. We improve this technique by combining and further developing techniques of non-redundant aperture masking and self-calibration from astronomy. Using visible synchrotron radiation, tests at the ALBA synchrotron show that this method provides an accurate two-dimensional beam characterisation, even in a single 1ms integration. The technique is resistant to phase fluctuations that might be introduced by vibration of optical components, or in the laboratory atmosphere.

INTRODUCTION

Two-dimensional (2D) beam size measurements in the transverse plane are of fundamental importance to quantify the performance of accelerators. They allow for the characterization of the emittance of the particle beam, a key parameter defining an accelerator. The transverse distribution of particles is well characterized by a 2D Gaussian [1] and parameterised by major axis, minor axis, and the tilt angle.

In synchrotron light sources, noninvasive beam size measurements exploiting the Synchrotron Radiation (SR) emitted by the electron beam are mainly performed via direct imaging or interferometry techniques [2]. Among the direct imaging techniques, the X-ray pin-hole [3] is widely used in synchrotron light sources as it directly provides a 2D image of the source.

At longer wavelengths the direct imaging is limited by diffraction and interferometric techniques are preferred. Among them, the two-aperture interferometer [4] is widely used in accelerators, but it only provides a one dimensional measurement in the direction of the orientation of the apertures. Full 2D beam reconstruction can be obtained by a series of measurements, rotating the aperture mask between measurements [5], but at least four orientations are needed. A four-aperture square interferometric mask layout [6] has been used to obtain a 2D source size from a single interferometric measurement, but such a mask layout suffers from decoherence due redundant sampling in Fourier space [7]. Moreover, the non-uniformity of aperture illumination across the mask due to the intrinsic distribution of the synchrotron

radiation might irrecoverably corrupt the results [8].

Non-redundant 2D aperture masks and 'gain fitting' to deal with non-uniform illumination are techniques broadly used in astronomy [9, 10]. We combine these two techniques and adapt them to apply to particle accelerators to reliably provide a full characterisation of the 2D beam in a single measurement using the visible part of the synchrotron radiation. In this paper we present the technique and use it to characterize the ALBA electron beam.

EXPERIMENTAL SETUP

The experiments were carried out at the ALBA synchrotron facility. The laboratory optical bench setup and the imaging camera were similar to the two-aperture interferometry described by [5], except that we use new multi-aperture masks and different integration times.

We present source size measurements made using a five-aperture mask designed such that the vector ('baseline') between every pair of apertures is unique (a 'non-redundant' mask). This means that each spatial frequency in the Fourier domain is measured by only a single pair of apertures in the plane of the mask, thereby avoiding decoherence that would occur for redundant aperture measurements in the presence of phase errors. This mask was an adaptation of the non-redundant array in [11], with the five apertures selected to maximize the longer baselines (given the source is only marginally resolved) while fitting within the illuminated area.

The geometry of the mask is shown in Figure 1. The

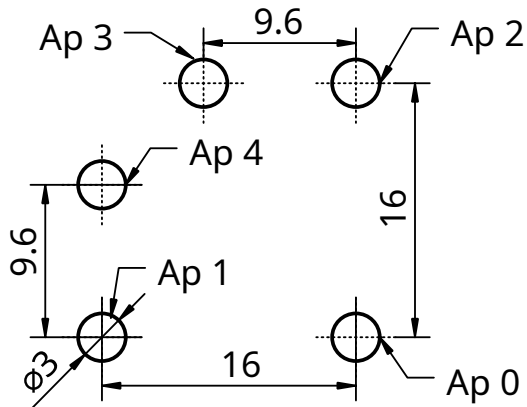


FIG. 1. Drawing of the non-redundant mask with aperture labels as used for labelling baselines. (All dimensions in millimetres).

hole sizes were 3mm in diameter and the mask was machined out of aluminium to high accuracy in the ALBA machine shop (better than 0.1 mm).

MEASURING VISIBILITIES

Data are acquired as CCD two-dimensional arrays of size 1296×966 . We first remove the constant offset which is due to a combination of the bias and the dark current. We use a fixed estimate of this offset obtained by examination of the darkest areas of the CCD, as well as from the FFT of the image. Errors in this procedure accumulate in the central part of the FFT and contribute to the overall uncertainty of the beam reconstruction.

Next we pad and center the data so that the centre of the Airy disk-like envelope of the fringes set by the hole diameter is in the centre of a larger two-dimensional array of size 2048×2048 . To find the correct pixel to center to, we first filter the acquired image with a wide (50 pixel) Gaussian kernel, then select the pixel with highest signal value. The Gaussian filtering removes the fringes leaving the remaining signal approximately corresponding to the fringe envelope. Without the filtering, the particular central pixel selected would be affected by the fringe position and the photon noise, rather than the envelope.

An example CCD frame processed in this way is shown in Figure 2. With five apertures arranged in a non-redundant layout the interference pattern is complex. The primary and first side lobe of the Airy disk envelope of the fringes can be seen. The measurement has high signal-to-noise with the fringes even in the first side-lobe clearly discernible above the noise.

To calculate the coherent power between the apertures,

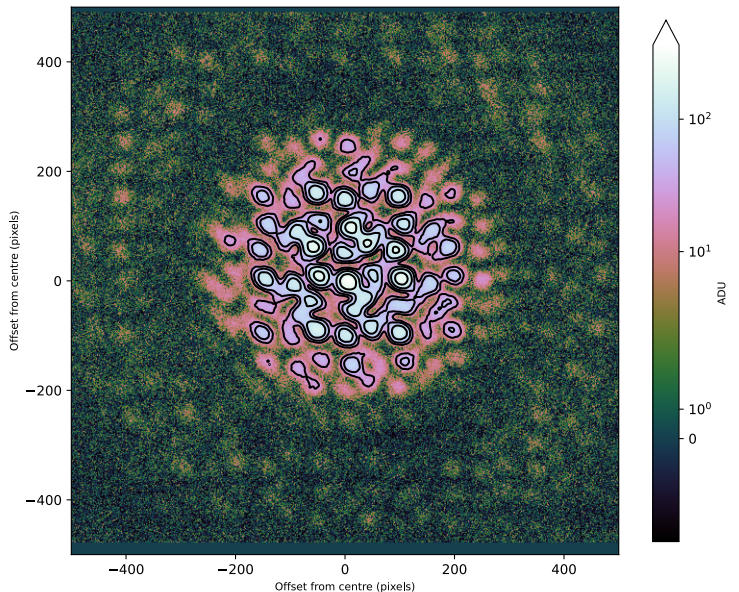


FIG. 2. Interferogram with five 3 mm-diameter holes and 1 ms integration time. The CCD image is bias-subtracted and centered. Contours are power-law in 2^{-n} .

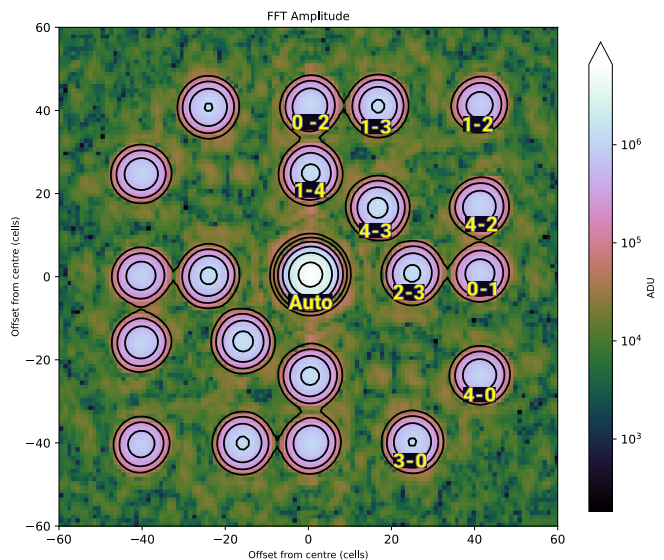


FIG. 3. Amplitude of the FFT of the sample interferogram in Figure 2, contours drawn at 2^{-n} intervals relative to image maximum. Labels identify peaks of amplitude with the pair of apertures forming the baseline of visibility that the peak represents.

i.e. the visibilities, we use the Fourier transform approximation of the van Cittert–Zernike theorem that the coherence and the image intensity are related by a Fourier transform. We therefore compute the two-dimensional Fourier transform of the padded CCD frame using the FFT algorithm. Amplitude of an example Fourier transform is shown in Figure 3. Distinct peaks can be seen in the FFT amplitude corresponding to each baseline (i.e., vector) between the apertures in the mask.

We extract the correlated power on each of the baselines by calculating the complex sum of pixels within a circular aperture of radius 7 pixels, centered at the calculated position of the baseline. With the array padding used here, 1 mm on the mask corresponds to 2.54 pixels in the Fourier transformed interferogram and the correlated signal is expected up to twice the hole radius so the 7 pixel aperture captures almost all of the signal while minimising noise and systematics. The resulting complex sum value contains both the amplitude and phase of the visibility.

FITTING THE COHERENCES

The measured visibilities are a function of both the degree of coherence and the amplitudes of the electromagnetic radiation passing through each of the apertures. Since it is not possible to ensure the intensity of radiation through the apertures are all the same, our strategy is to simultaneously fit for both the coherences as well as the ‘gains’, $\|G_i\|$, corresponding to the square root of intensity of the incident radiation at each of the apertures. If this fitting is not performed, errors introduced by non-uniform illumination are greater in the multi-aperture interferometry than in the two-aperture case because we only have a constraint on the total power of the radiation through all the apertures, not on the particular two apertures forming each visibility. This means that without fitting, a fractional difference in illumination of ϵ leads to an error in coherence of order ϵ^2 in the two-aperture case but order ϵ in the multi-aperture case.

Parametrisation of the model for the coherence

By the van Cittert–Zernike theorem the coherence can be very well represented by the Fourier transform of the source intensity distribution. Working on the assumption that the source is a multi-variate Gaussian [1], then the coherence is also a multi-variate Gaussian, which is what we use as the model. We fit a parametrisation in terms of the overall width (σ) and the distortion in the vertical-horizontal directions (η) and diagonal (ρ) directions:

$$\gamma(u, v) = \exp\left[-\frac{(u^2 + v^2) + 2\rho(uv) + \eta(u^2 - v^2)}{2\sigma^2}\right] \quad (1)$$

In this parametrisation the major and minor axes are $(1 - \sqrt{\eta^2 + \rho^2})^{-\frac{1}{2}}$ and $(1 + \sqrt{\eta^2 + \rho^2})^{-\frac{1}{2}}$ times the σ parameter. This is a convenient parametrisation for fitting as it avoids trigonometric functions and has low covariance of parameters in typical situations.

Likelihood function

The predicted visibility amplitudes $\|V_{ij}\|$ and the predicted total signal $\|V_{\text{auto}}\|$ are related to the model coherence $\gamma(u_{ij}, v_{ij})$ on a baseline (u_{ij}, v_{ij}) and to the ‘gain’ of each aperture, $\|G_i\|$ (again, the square root of intensity through the aperture), by:

$$\|V_{ij}\| = \gamma(u_{ij}, v_{ij})\|G_i\|\|G_j\| \quad (2)$$

$$\|V_{\text{auto}}\| = \sum_i \|G_i\|^2. \quad (3)$$

Under the assumption of normally distributed uncorrelated errors in the visibility measurements the likelihood is then:

$$-\log(L) = \frac{\|V_{\text{auto}}^{\text{obs}} - V_{\text{auto}}^{\text{mod}}\|^2}{\xi_{\text{auto}}} + \sum_{i=0}^{N-2} \sum_{j=i+1}^{N-1} \frac{\|V_{ij}^{\text{obs}} - V_{ij}^{\text{mod}}\|^2}{\xi_{\text{vis}}} \quad (4)$$

where, N is the number of apertures in the mask (5 in this case), and ξ_{auto} and ξ_{vis} are the noise estimates for total power and the visibilities, respectively. We estimated ξ_{vis} by measuring visibilities in apertures of the same size as the true visibilities but positioned away from any real coherent signal in Figure 3. For ξ_{auto} we estimate additional 1% of the total power signal error due to systematic effects such as the bias subtraction.

Minimisation procedure

The best-fitting model was found by maximising the likelihood using the Levenberg–Marquardt algorithm with a numerically evaluated Jacobian. The fitting processing time is dominated by the Fourier transform computations and can be completed in around 25ms on a server-class CPU (dual Intel Xeon 8276), faster than the typical CCD read-out time. This means that, although in present experiments we analysed the data offline, the technique could be used for a system implemented for beam characterisation with low and predictable latencies typically dominated by the fixed latency of the CCD readout, i.e., near real-time measurement.

RESULTS

We obtained a number of measurement runs on 2023-06-14 with 3 mm and 5 mm apertures, and with 1 ms and

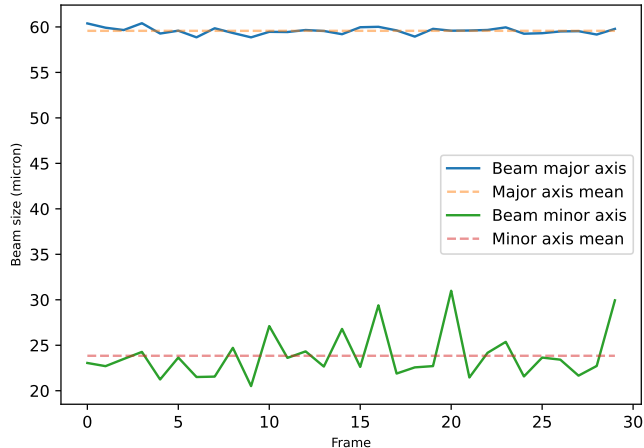


FIG. 4. Time series of measured beam major and minor axes, σ , from 30 interferogram frames each separated by one second. Dash lines are mean values.

3 ms integration times. Each run consisted of 30 CCD frames separated by one second. Data with 3 mm apertures and 1 ms integration time have the least time variation and highest apparent coherences indicating that it is of best quality [7].

Beam size measurement

Using the 1 ms integration time data, we analysed each frame to derive both the illumination through each mask hole and the best fitting values for the coherences. The coherences are then used to calculate the electron beam source size. The time series of these measurements, shown in Figure 4, show high stability and repeatability, with an rms scatter of $0.4 \mu\text{m}$ and $2.6 \mu\text{m}$ in beam major and minor axes, respectively, and 0.9° in the angle.

The final beam derived is the average of the time series, which is shown in Figure 5. The mean estimate of the axes sizes is $\sigma_{\text{major}} = 59.6 \mu\text{m} \pm 0.1 \mu\text{m}$ and $\sigma_{\text{minor}} = 23.8 \mu\text{m} \pm 0.5 \mu\text{m}$. The error on the minor axis is larger because of its significantly smaller size, and also because the available baselines are shorter, being limited by the size of the illuminated region. The angle the major axis makes with the horizontal is $15.9^\circ \pm 0.2^\circ$.

We find a significant difference between the $\|G_i\|$ values of different mask holes (by around 25%), which are due to unavoidable differences in the illumination from the beam across the mask. This is due to the inherent vertical intensity distribution of the synchrotron light, plus the Fraunhofer diffraction produced by the mirror edges. We find the $\|G_i\|$ values are stable over the time series to better than 1%. These results demonstrate the importance of fitting for both $\|G_i\|$ values and coherences.

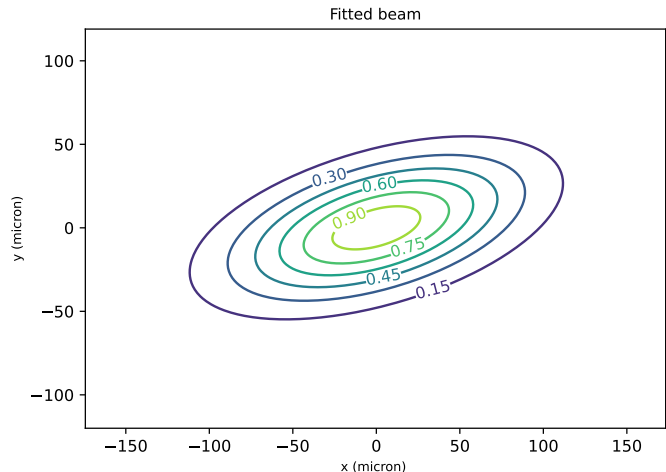


FIG. 5. Full 2D beam reconstruction from the average of 30 frames each 1 ms integration time.

Comparison to rotated two-aperture SRI

On the same day we also obtained measurements using rotated two-aperture SRI as described by [5]. This method has previously been shown to be reliable and uses a different fitting procedure to obtain the beam sizes. Those measurements were obtained with 3 ms integration time (in order to achieve similar SNR with less overall light throughput), and so we compare them against the analysis of the five-aperture interferometry in Table I. As for the 5 apertures, the two-aperture SRI measurements employed 30 consecutive frames in each of four rotated positions of the mask. These rotated positions are required to perform the full 2D characterization in this method.

Table I also shows the expected results for horizontal and vertical beam size and the tilt angle at the synchrotron radiation extraction point obtained using Linear Optics from Closed Orbits (LOCO, [12]). LOCO is a tool to measure and correct the orbit of a circular accelerator. It takes into account several measurements of the machine, such as current in magnets, and models them to estimate the expected beam behavior. The obtained result is not necessarily exact but indicative, since it is impossible to parameterize all the instrumentation.

Table I shows consistency within the errors between the 5-hole and 2-hole beam size measurements. The SRI measurements are also within 4% to 20% of the LOCO modeling, depending on parameter. We also list the X-ray pinhole measurements, which are consistent within the errors with the SRI values, although the X-ray measurement is made at a different location in the system and hence a direct comparison may not be warranted.

Method	Major (μm)	Minor (μm)	Tilt Angle
2ap (3 ms)	61.7 ± 1.5	25.5 ± 1.5	16.6°
5ap (1 ms)	59.6 ± 0.1	23.8 ± 0.5	$15.9^\circ \pm 0.2^\circ$
LOCO	57.5	20.6	14.9°
Pinhole	58.5	24.6	14.9°

TABLE I. Comparison of beam size measurements by various methods. 2ap: two-aperture rotated mask. 5ap: the present five-aperture method. LOCO: ideal value based on the analysis of the magnet lattice of ALBA [12]. Pinhole: beam size inferred from the emittance calculation at the ALBA x-ray pinholes, although at a different location in the ring [13].

CONCLUSIONS

The synchrotron beam can be well-characterised from a single interferogram made with a simple apparatus with no moving parts. The relatively large CCD image data set can be processed without iterative model-fitting to derive a much smaller data set of visibilities (in our case 10), which are then input into a fitting procedure. Importantly, this model fitting needs to fit for both the differential illumination of the apertures as well as for the coherences. The overall processing complexity is low and suitable for near-real time applications. The beam parameters and uncertainty in a single acquisition with a 5-hole non-redundant mask are comparable to those obtained with the two-aperture method employing multiple acquisitions with rotation of the aperture. The larger amount of light let through by the five apertures contributes to the efficiency of the technique. Good results can be obtained with apertures small enough and integration times short enough that there do not seem to be pronounced de-correlation effects.

The technique requires a Gaussian assumption for the beam shape, although this assumption appears well justified based on X-ray pinhole imaging [13]. In order for the model and the $\|G_i\|$ values to be well constrained, there must be more measured visibilities than the sum of the number of apertures and the number of model free parameters [10]. This is satisfied with 5 apertures for the Gaussian model of the synchrotron beam. More complex models are possible, e.g., in astronomical applications it is also routine to iteratively build up a model when there is a significant number of measurements and the source plane can be assumed to be sparse [10]. In these cases, a larger number of apertures would be needed.

The technique presented can likewise be used for efficient and rapid characterisation of other high-intensity light sources even after propagation through a medium inducing phase and amplitude fluctuations. Moreover, the complex visibilities and $\|G_i\|$ values encode precise information on the optical performance of the system. The technique is a good demonstration interdisciplinary science, applying astronomical interferometric techniques

to accelerator physics.

Acknowledgments. The National Radio Astronomy Observatory is a facility of the National Science Foundation operated under cooperative agreement by Associated Universities, Inc. Patent applied for: UK Patent Application Number 2406928.8, USA Applications No. 63/648,303 (RL 8127.306.USPR) and No. 63/648,284 (RL 8127.035.GBPR)..

* E-mail:bn204@cam.ac.uk

† E-mail: uiriso@cells.es

- [1] M. Sands, The Physics of Electron Storage Rings: An Introduction, Conf. Proc. C **6906161**, 257 (1969).
- [2] G. Kube, Review of Synchrotron Radiation Based Diagnostics for Transverse Profile Measurements, in *Proceedings of DIPAC07, Venice (Italy)* (2007).
- [3] P. Elleaume, C. Fortgang, C. Penel, and E. Tarazona, Measuring Beam Sizes and Ultra-Small Electron Emittances Using an X-ray Pinhole Camera, *Journal of Synchrotron Radiation* **2**, 209 (1995).
- [4] T. Mitsuhashi, Beam profile and size measurement by SR interferometers, in *Joint US-CERN-Japan-Russia School on Particle Accelerators: Beam Measurement* (1998) pp. 399–427.
- [5] L. Torino and U. Iriso, Transverse beam profile reconstruction using synchrotron radiation interferometry, *Phys. Rev. Accel. Beams* **19**, 122801 (2016).
- [6] M. Masaki and S. Takano, Two-dimensional visible synchrotron light interferometry for transverse beam-profile measurement at the SPring-8 storage ring, *Journal of Synchrotron Radiation* **10**, 295 (2003).
- [7] C. Carilli, B. Nikolic, L. Torino, U. Iriso, and N. Thyagarajan, *Deriving the size and shape of the ALBA synchrotron light source with optical aperture masking: technical choices*, Tech. Rep. (ALBA, 2024).
- [8] A. Novokshonov, G. Kube, and A. Potylitsyn, Two-Dimensional Synchrotron Radiation Interferometry at PETRA III, in *8th International Particle Accelerator Conference* (2017).
- [9] C. A. Haniff, C. D. Mackay, D. J. Titterton, D. Sivia, and J. E. Baldwin, The first images from optical aperture synthesis, *Nature* **328**, 694 (1987).
- [10] F. R. Schwab, Processing of three-dimensional data, in *1980 International Optical Computing Conference I*, Society of Photo-Optical Instrumentation Engineers (SPIE) Conference Series, Vol. 231, edited by W. T. Rhodes (1980) p. 18.
- [11] A. I. González and Y. Mejía, Nonredundant array of apertures to measure the spatial coherence in two dimensions with only one interferogram, *J. Opt. Soc. Am. A* **28**, 1107 (2011).
- [12] J. Safranek, Experimental determination of storage ring optics using orbit response measurements, *Nuclear Instruments and Methods in Physics Research Section A: Accelerators, Spectrometers, Detectors and Associated Equipment* **388**, 27 (1997).
- [13] U. Iriso, Z. Marti, A. Nosych, A. Cazorla, and I. Mases, PSF Characterization of the ALBA X-Ray Pinholes, in

